Journal of Alloys and Compounds 509 (2011) 5637–5640

Contents lists available at ScienceDirect

Journal of Alloys and Compounds

journal homepage: www.elsevier.com/locate/jallcom

Relationship between structure and properties in high-temperature $Bi(Al_{0.5}Fe_{0.5})O_3$–$PbTiO_3$ piezoelectric ceramics

Zhonghua Yao[a,*], Liyuan Peng[b], Hanxing Liu[b,*], Hua Hao[b], Minghe Cao[b], Zhiyong Yu[b]

[a] Key Laboratory of Advanced Technology for Specially Functional Materials, Ministry of Education, Wuhan University of Technology, Wuhan 430070, PR China
[b] State Key Laboratory of Advanced Technology for Materials Synthesis and Processing, Wuhan University of Technology, Wuhan 430070, PR China

ARTICLE INFO

Article history:
Received 17 December 2010
Received in revised form 18 February 2011
Accepted 19 February 2011
Available online 26 February 2011

Keywords:
Ceramics
X-ray diffraction
Dielectric properties
Piezoelectric properties
BAF–PT ceramics

ABSTRACT

Ceramic samples of $x\mathrm{Bi}(\mathrm{Al}_{0.5}\mathrm{Fe}_{0.5})\mathrm{O}_3$–$(1-x)\mathrm{PbTiO}_3$ (BAF-PT, $x = 0.05$–0.5) solid solutions were fabricated using the conventional solid state reaction method. X-ray diffraction analysis revealed that all compositions can form single perovskite phase with tetragonal symmetry. The relationship between the tetragonal lattice parameters, tetragonality c/a, cell volume, and ferro-piezoelectric characterization as a function of x was systematically investigated. The BAF modification can effectively improve the poling condition at a proper BAF content. A combination of piezoelectric constant of d_{33} (50–60 pC/N), electromechanical planar coupling coefficients of k_p (20.3–22.5%), and high Curie temperature T_c (>478 °C) suggested that BAF–PT could be a good candidate for high-temperature piezoelectric applications.

1. Introduction

Piezoelectric ceramics based on the perovskite $\mathrm{Pb}(\mathrm{Zr}_{1-x}\mathrm{Ti}_x)\mathrm{O}_3$ (PZT) system are widely used as sensors and actuators because of their excellent dielectric, piezoelectric, and electrostrictive properties [1–11]. However, the major disadvantage of PZT ceramics is the relatively low Curie temperatures T_c (~300 °C). This low T_c comes with the disadvantages of more temperature-dependent properties and less polarization stability, which in turn restricts the operating temperature range (~$1/2T_c$) to less than 150 °C. Technological advancements in structure and control systems integration have created the need for the use of piezoelectric materials at higher temperatures (>200 °C) in applications such as structural health monitoring and engine knock control. Recently, a new binary Bi-based system has been found to have a morphotropic phase boundary (MPB) with high transition temperatures and high electromechanical properties [12–29]. Among these binary system, $\mathrm{BiScO_3}$–$\mathrm{PbTiO_3}$ (BS–PT) was found to have a MPB and achieved more attention, as they own relatively high transition temperature (450 °C) and the modest piezoelectric properties, being suitable for some of the applications, comparable to the doped PZT ceramics [17,23]. However, the disadvantage of this material is the high cost of $\mathrm{Sc_2O_3}$ which means that the production of BS–PT ceramics is not economically viable.

Since the high cost of BS–PT prohibits its commercial applications, a substitute for $\mathrm{Sc_2O_3}$ has been required. Recently, some studies have been focused on some inexpensive metal oxides to replace the above expensive scandium oxides to form new solid solutions, such as $\mathrm{Fe_2O_3}$, $\mathrm{Al_2O_3}$, and so on [24,30]. $\mathrm{BiFeO_3}$–$\mathrm{PbTiO_3}$ (BF–PT) exhibits a MPB at 30 mol% of $\mathrm{PbTiO_3}$ between a tilted rhombohedral ($R3c$) and a tetragonal phase ($P4mm$) phase [30]. Several studies have reported that the MPB composition in BF–PT system has a high T_c (650 °C), but to date high ferroelectric/piezoelectric measurements have proven to be difficult, possibly due to the usually large c/a ratio (1.17) in the tetragonal phase close to the MPB and/or its high conductivity [31–35].

There are many activities at present on studying the effect of the doping in ferroelectric materials to increase the resistivity and reduce the coercive field [36]. The deleterious side of this doping, however, is a drastic reduction in the Curie point, and therefore, the decrease of the maximum operating temperature. The general trend showing the increase of T_c with increasing c/a ratio holds for all systems presented, with a variety of chemistries, including systems with barium, cadmium, sodium, lanthanum, potassium and bismuth on the A-site [37]. When coupled with the spontaneous piezoelectric strain limit, high Curie temperature materials should exhibit large c/a ratios and correspondingly a large piezoelectric strain. Interestingly, Ranjan and co-workers [38] found that unlike $\mathrm{BiScO_3}$–$\mathrm{PbTiO_3}$, the MPB composition could not be achieved in $\mathrm{BiAlO_3}$–$\mathrm{PbTiO_3}$ (BA–PT) and retained high Curie point of pure $\mathrm{PbTiO_3}$ despite the decrease in the tetragonality c/a possibly due to the compensated stability energy by Bi ions.

---

* Corresponding authors. Tel.: +86 2787864681; fax: +86 2787879468.
E-mail addresses: yaozhhua@whut.edu.cn (Z. Yao), lhxhp@whut.edu.cn (H. Liu).

0925-8388/$ – see front matter © 2011 Elsevier B.V. All rights reserved.
doi:10.1016/j.jallcom.2011.02.106

In the past, most investigations were mainly focused on the composition near MPB for perovskite piezoelectric system because of its excellent electrical properties in this region. However, BF–PT compositions close to MPB region exhibit high leakage current and are not easy to be effectively poled. As for BA–PT, the MPB composition could not be achieved due to the limited solid solubility [38]. Here, we focused on the ternary compositions with the formula of $Bi(Al_{0.5}Fe_{0.5})O_3$–$PbTiO_3$ through the substitution of Sc^{3+} ion by $(Al_{0.5}Fe_{0.5})^{3+}$ complex ions and wanted to improve the poling behavior by the modification. As discussed above, high Fe^{3+} content can result in high leakage current and/or low resistivity, making it difficult to be used. The aim of doping is to improve the poling condition and decrease the leakage current. So, the present work is initiated by this motivation to further study the relationship between structure and properties in the compositions with low Fe^{3+} content in the $Bi(Al_{0.5}Fe_{0.5})O_3$–$PbTiO_3$ system.

2. Experimental

Specimens with the compositions of $x\mathrm{Bi}(Al_{0.5}Fe_{0.5})O_3$–$(1-x)PbTiO_3$ (BAF–PT, $x = 0.05$–0.50) were prepared by conventional solid-state synthesis. The reagent-grade materials of Bi_2O_3, Fe_2O_3, PbO, TiO_2, and Al_2O_3 were weighed as starting powders according to the nominal compositions, with 1.0 wt.% excess amounts of Bi_2O_3 and PbO to compensate the volatilization during sintering. The powders were re-mixed, calcined, ground, dried and then mixed with polyvinyl alcohol (PVA) binder. The powders were pressed into pellets with 12 mm in diameter and 1.2 mm in thickness at 180–200 MPa. These pellets were burnt out at 600 °C and sintered at 1050–1200 °C for 2 h with PbO and Bi_2O_3 atmosphere to prevent their volatilization during densification.

Phase structures were detected by a Philips vertical X-ray diffractometer (XRD, PW3050/60, MPSS) using Cu Kα1 radiation confirmed the formation of perovskite-type phases with no evidence of any impurities, 2θ in the range of 10–60° with a step of 0.02°. The lattice parameters were calculated by X'Pert HighScore Plus software. For electrical measurement, the pellets were printed on both sides by silver electrodes with a diameter smaller than that of test specimens, fired at 500 °C for 20 min, and poled in an oil bath under an electric field (>4 kV/mm) at 120 °C for 15 min. By using electrodes with a diameter smaller than that of the ceramic test specimens, one could ensure that when dielectric breakdown did occur, it was through the ceramic rather than around the edge. Temperature frequency dependence of dielectric properties of the unpoled samples was measured using an Agilent precision LCR meter (E4980A) from room temperature to 600 °C. The piezoelectric constant d_{33} and electromechanical planar coupling coefficients k_p were measured one day after poling using a quasi-static piezoelectric d_{33} meter (Model ZJ-3D, Institute of Acoustics Academic, and Beijing, China) and an impedance analyzer (HP4294A) by the resonance and anti-resonance technique on the basis of IEEE standards, respectively [39]. The room-temperature hysteresis loops of polarization were performed using RT66A testing system (Radiant Technologies) in silicon oil under a saturated field without breakdown.

3. Results and discussion

Fig. 1 shows the room temperature X-ray diffraction patterns of the BAF–PT ceramics as a function of doping concentration. The splitting of diffraction peaks of (0 0 2)/(2 0 0) is a symbol of tetragonal symmetry. It is quite evident that all compositions exhibit a single tetragonal symmetry and a second phase is starting to appear when $x = 0.50$. It can be indexed by typical tetragonal perovskite structure.

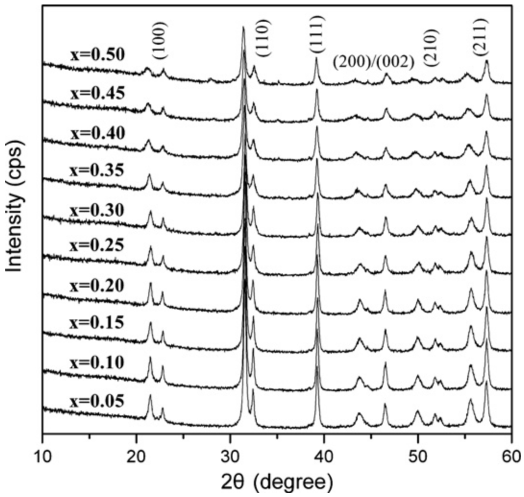

Fig. 1. Room temperature X-ray diffraction patterns of the BAF–PT ceramics as a function of doping concentration.

Fig. 2 shows the variation of the tetragonal lattice parameters, tetragonality c/a and cell volume of the ceramic samples as a function of x. As shown, lattice constant does not increase monotonically with increasing x value, but shows fluctuation. As x increases, the tetragonality decreases at $x \leqq 0.25$ and then increases at $x > 0.25$, indicative of the variation of crystal structure. It has been reported that BF substitution can increase the tetragonality while BA substitution can firstly decrease and then increase the tetragonality in a limited composition range [30,38]. The cell parameter c exhibits the same trend as the tetragonality. The cell volume follows the trend like the tetragonality except for the composition range $0.15 \leqq x \leqq 0.30$. Here, Bi^{3+} (1.17 Å for CN = 8), Al^{3+} (0.535 Å for CN = 6), Fe^{3+} (0.61 Å for CN = 6, low spin), Pb^{2+} (1.29 Å for CN = 8), and Ti^{4+} (0.605 Å for CN = 6), respectively [40]. The reduction of cell volume at low x can be ascribed to the ionic size effect, where the ion radius of Bi^{3+} and Al^{3+} are less than that of Pb^{2+} and Ti^{4+}, respectively. An enhancement in the tetragonality and cell volume is seen towards BAF-rich compositions, which is in agreement with the behavior observed in the BF–PT ceramics [30,41]. This increase can be ascribed to the difference of ion radius that the ionic radius of Fe^{3+} is larger than that of Ti^{4+}, which will break the rise of the volume at BAF-rich compositions. In fact, the abnormal volume in the composition $0.15 \leqq x \leqq 0.30$ can also be related to the larger Fe^{3+}, where the substitution can result in the increase of a and the decrease of c. The unit cell volume of tetragonal phase can be calculated by $a \times b \times c$, which can be responsible for the abnormal cell volume. Qi et al. [42] have demonstrated that tetragonality is strongly coupled to the B-cation displacement and weakly coupled to the A-cation displacement in the $PbTiO_3$-derived ferroelectric perovskite solid solutions. Examination of various $BiM^{3+}O_3$ additives to $PbTiO_3$ for different M^{3+} ionic sizes revealed that substitution of either small B cations or low doping of large B cations gives rise to large spontaneous polarization and tetragonality. Here, the low doping of $(Al_{0.5}Fe_{0.5})^{3+}$ cations can give rise to high tetragonality, while high tetragonality can also be obtained at high doping level. The origin of this discrepancy is not known. It should be noted, however, the decrease of tetragonality can improve poling conditions for the decrease in coercive field, possibly as a new high-temperature candidate available.

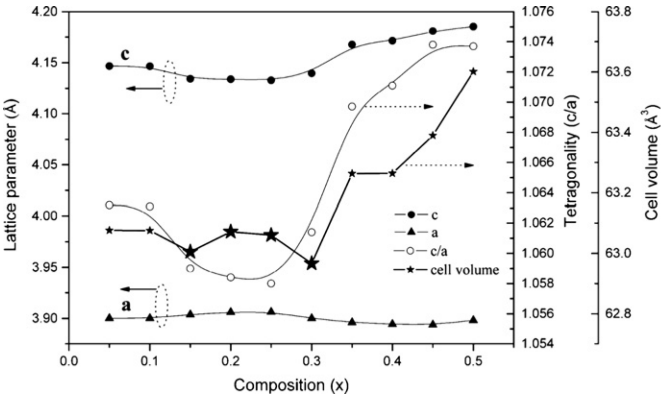

Fig. 2. The variation of the tetragonal lattice parameters, tetragonality c/a and cell volume as a function of x.

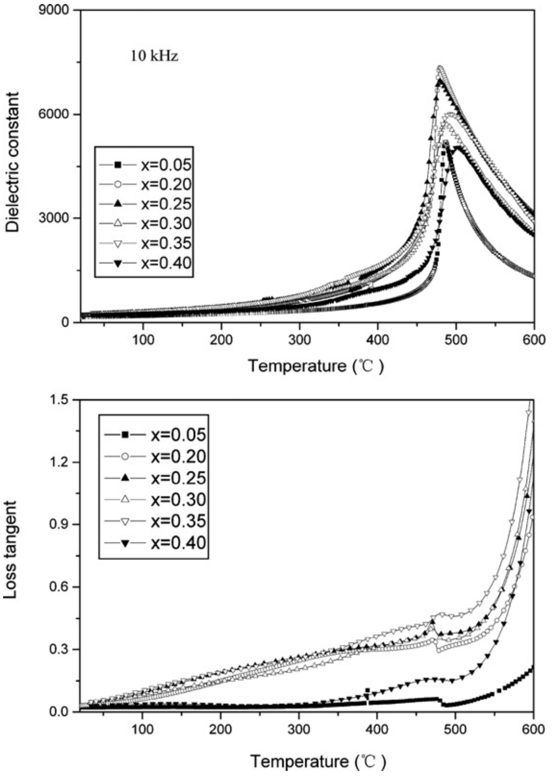

Fig. 3. Dielectric properties of the BAF–PT ceramics at 10 kHz as a function of temperature.

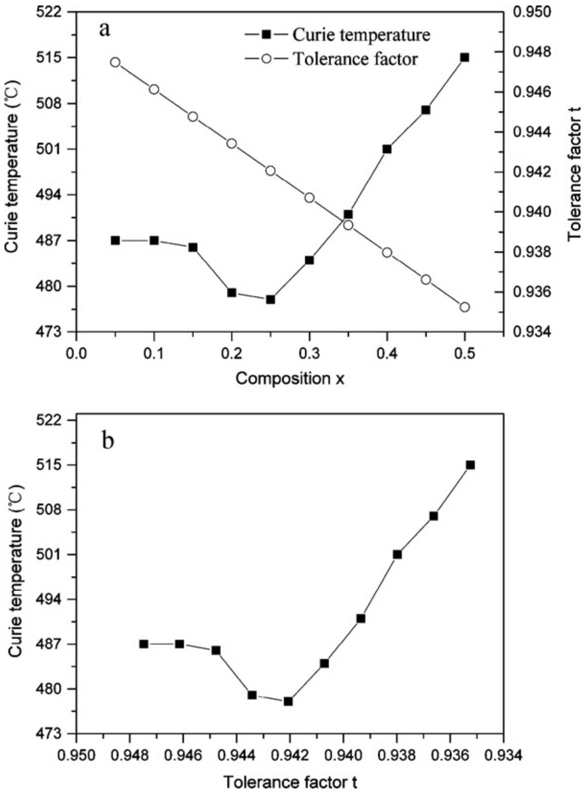

Fig. 4. The relationship between Curie point and tolerance factor *t* as a function of composition *x* for the BAF–PT system.

Fig. 3 shows dielectric properties of the BAF–PT ceramics at 10 kHz as a function of temperature. All compositions show the ferroelectric–paraelectric phase transformation determined from sharp dielectric peaks. It is well-known that Curie point T_c is tightly related to the tetragonal symmetry for a perovskite-structured composition, namely that high tetragonality owns high transition temperature. For $x = 0.05$ at 10 kHz, a ferroelectric to paraelectric phase transition was apparent at 487 °C, as shown by the sharp frequency independent maximum of dielectric constant and the associated peak in loss. Above T_c, the losses increased dramatically because of increasing conductivity [43].

It is well known that the Curie point is closely related to structural displacements and/or the tetragonality. The degree of distortion of the perovskite structure can be determined by the tolerance factor *t*, $t = (r_A + r_O)/\sqrt{2}(r_B + r_O)$, where r_A, r_B, and r_O are the average ionic radii of the A and B-site cations, and an oxygen ion, respectively. Fig. 4 shows the relationship between Curie point, and tolerance factor *t* as a function of composition *x* for the BAF–PT system at 10 kHz. The Curie point shown in Fig. 4(a) decreases up to $x = 0.25$ and then increases sharply with increasing *x*, similar to the trend of the tetragonality and tolerance factor. As observed from these results, the lowest Curie point can be obtained at $x = 0.25$ (478 °C) due to the lowest tolerance factor and tetragonality. Theoretically, the atomic displacements along the polar axis and/or the titling of the centre octahedron of the perovskite are smaller so that the lattice energy involved is lowered. Therefore, the low atomic displacement means low lattice energy, indicative of low transition temperature. The variation of Curie temperature is tightly consistent with the above theoretical analysis, as shown in Fig. 4(b). It can be seen that all the compositions exhibit high transition temperature above 478 °C, comparable to the MPB BS–PT (∼450 °C).

Fig. 5 shows the ferroelectric hysteresis loops obtained for BAF–PT ceramics under applied electrical fields without breakdown. It can be observed that all the specimens exhibit some conductive behavior, especially for the compositions with high BAF doping level. With an increasing BAF doping level, the shapes of the hysteresis loop gradually become round and conductive. This implies that the leakage current for BAF–PT ceramics increases by the modification of BAF. On the other hand, remnant polarization P_r for BAF–PT ceramics monotonically increases with the increase in *x* from 0.05 to 0.25, and then fluctuates with further increase of *x* due to conductive characterization. Theoretically, high titling of perovskite octahedron should exhibit high strain or ferroelectric characterization for a certain composition. However, high tetragonality needs high poling field to rotate the polar dipoles. Here,

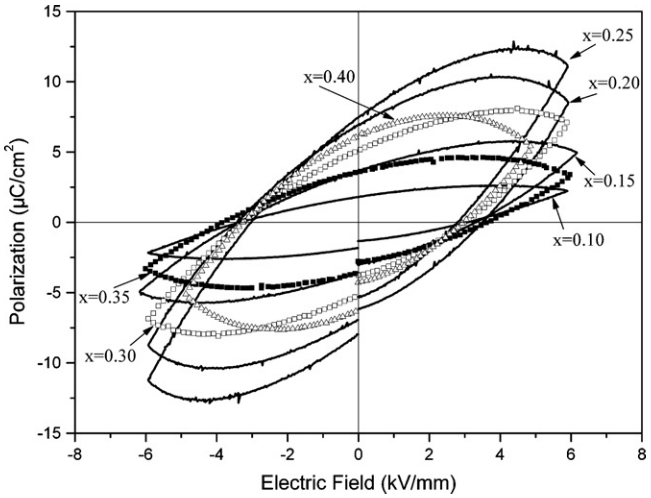

Fig. 5. Ferroelectric hysteresis loops obtained for BAF–PT ceramics under applied electrical fields without breakdown.

high and/or very low BAF modification can retain high tetragonality which makes the poling difficult. Normal ferroelectric hysteresis loops for high modification ($x > 0.40$) cannot be obtained due to high leakage current and/or high coercive field, indicating that a much higher saturated polarization can be expected. The composition with high tetragonality exhibits low piezoelectric constant d_{33} (>30 pC/N) due to the limited poling field. The compositions $x = 0.20$ and 0.25 with relative low tetragonality shows a piezoelectric constant d_{33} in the range of 50–60 pC/N and an electromechanical planar coupling coefficients k_p in the range of 20.3–22.5%, indicative of the effective improvement of poling behavior. As a result, the proper introduction of BAF can properly reduce the leakage current and improve the ferroelectric properties, making the poling easier, and therefore the piezoelectric properties of BAF–PT ceramics can be effectively measured.

4. Conclusions

The relationship between structure and electrical properties of $x\text{Bi}(\text{Al}_{0.5}\text{Fe}_{0.5})\text{O}_3$–$(1-x)\text{PbTiO}_3$ (BAF–PT, $x = 0.05$–0.5) solid solutions was systematically investigated. BAF–PT ceramics exhibited single tetragonal crystal structure at room temperature, indicating better homogeneity and the formation of compounds. BAF modification in PT exhibited many interesting features, such as abnormal shift of Curie temperature, fluctuation of lattice constant, and the improvement of poling condition. The results indicated that Curie point was tightly related with the tetragonality. The optimal electrical properties can be obtained in the composition $x = 0.20$–0.25 with $d_{33} = 50$–60 pC/N, $k_p = 20.3$–22.5%, and high Curie point ($T_c > 478\,^\circ\text{C}$), indicative of a promising ferroelectric candidate for high-temperature piezoelectric transduction applications.

Acknowledgements

The authors would like to thank the support of Key Programmer of Natural Science Foundation of China (No. 50932004), Natural Science Foundation of China (No. 50872102), the Key Grant Project of Chinese Ministry of Education (No. 309022), and the Fundamental Research Funds for the Central Universities (No. 2010-IV-045).

References

[1] B. Jaffe, W.R. Cook, H. Jaffe, Journal of Piezoelectric Ceramics, Academic Press, New York, 1971.
[2] S.K. Pandey, O.P. Thakur, D.K. Bhattacharya, C. Prakash, R. Chatterjee, J. Alloys Compd. 468 (2009) 356.
[3] J.N. Wang, L.D. Wang, W.L. Li, W.D. Fei, J. Alloys Compd. 509 (2011) 3347.
[4] C.A. Randall, A. Kelnberger, G.Y. Yang, R.E. Eitel, T.R. Shrout, J. Electroceram. 14 (2005) 177.
[5] N. Vittayakorn, G. Rujijanagul, D. Cann, J. Alloys Compd. 440 (2007) 259.
[6] Q.L. Zhao, M.S. Cao, J. Yuan, W.L. Song, R. Lu, D.W. Wang, D.Q. Zhang, J. Alloys Compd. 492 (2010) 264.
[7] Y. Cheng, Y. Yang, Y. Wang, H. Meng, J. Alloys Compd. 508 (2010) 364.
[8] S.Q. Zhang, W.D. Fei, W.L. Li, J.N. Wang, J. Alloys Compd. 487 (2009) 703.
[9] Z. Cao, G. Li, S. Or, J. Zeng, L. Zheng, Q. Yin, J. Alloys Compd. 496 (2010) 13.
[10] D. Shim, J. Pak, K. Nam, G. Park, J. Alloys Compd. 449 (2008) 32.
[11] B.W. Chua, L. Lu, M.O. Lai, G.H.L. Wong, J. Alloys Compd. 381 (2004) 272.
[12] C.J. Stringer, T.R. Shrout, C.A. Randall, I.M. Reaney, J. Appl. Phys. 99 (2006) 024106.
[13] Z.H. Yao, H.X. Liu, M.H. Cao, H. Hao, J. Appl. Phys. 109 (2011) 014105.
[14] C.A. Randall, R.E. Eitel, T.R. Shrout, D.I. Woodward, I.M. Reaney, J. Appl. Phys. 93 (2003) 9271.
[15] Y. Chen, J. Zhu, D. Xiao, B. Qin, Y. Jiang, J. Alloys Compd. 470 (2009) 420.
[16] Q.A. Zhang, Z.R. Li, Z. Xu, X. Yao, Ferroelectrics 408 (2010) 91.
[17] R.E. Eitel, C.A. Randall, T.R. Shrout, S.E. Park, Jpn. J. Appl. Phys. 41 (2002) 1999.
[18] G. Yu, X. Dong, G. Wang, F. Cao, X. Chen, J. Alloys Compd. 500 (2010) 56.
[19] S.M. Choi, C.J. Stringer, T.R. Shrout, C.A. Randall, J. Appl. Phys. 98 (2005) 034108.
[20] R. Rai, A.L.K.S. Sharma, J. Alloys Compd. 506 (2010) 815.
[21] G. Feng, R. Hong, J. Liu, L. Zhen, L. Cheng, C. Tian, J. Alloys Compd. 475 (2009) 619.
[22] H. Yamazaki, T. Shimura, W. Sakamoto, T. Yogo, J. Ceram. Soc. Jpn. 118 (2010) 631.
[23] R.E. Eitel, C.A. Randall, T.R. Shrout, P.W. Rehrig, W. Hackenberger, S.E. Park, Jpn. J. Appl. Phys. 40 (2001) 5999.
[24] R. Rai, A. Kholkin, S. Pandey, N.K. Singh, J. Alloys Compd. 488 (2009) 459.
[25] Z.H. Yao, H.X. Liu, Y. Liu, Z.H. Wu, M.H. Cao, H. Hao, Appl. Phys. Lett. 92 (2008) 142905.
[26] R. Rai, A. Sinha, S. Sharmac, N.K.P. Sinha, J. Alloys Compd. 486 (2009) 273.
[27] Z.H. Yao, H.X. Liu, M.H. Cao, H. Hao, J. Alloys Compd. 505 (2010) 281.
[28] R.R. Duan, R.F. Speyer, E. Alberta, T.R. Shrout, J. Mater. Res. 19 (2004) 2185.
[29] S.J. Zhang, R.E. Eitel, C.A. Randall, T.R. Shrout, E.F. Alberta, Appl. Phys. Lett. 86 (2005) 262904.
[30] D.I. Woodward, I.M. Reaney, R. Eitel, J. Appl. Phys. 94 (2003) 3313.
[31] S.A. Fedulov, P.B. Ladyzhinskii, I.L. Pyatigorskaya, Y.N. Venevtsev, Sov. Phys. Solid State 6 (1964) 375.
[32] S.A. Fedulov, Y.N. Venevstev, G.U. Zhdanov, Sov. Phys. Crystallogr. 7 (1962) 62.
[33] J.R. Cheng, W.Y. Zhu, N. Li, Mater. Lett. 57 (2003) 2090.
[34] R.T. Smith, G.D. Achenbach, R. Gerson, W.J. James, J. Appl. Phys. 39 (1968) 70.
[35] M.M. Kumar, V.R. Palkar, K. Srinivas, S.V. Suryanarayana, Appl. Phys. Lett. 76 (2000) 2764.
[36] J.R. Cheng, L.E. Cross, J. Appl. Phys. 94 (2003) 5188.
[37] S.C. Abrahams, S.K. Kurtz, P.B. Jamieson, Phys. Rev. 172 (1968) 551.
[38] A.K. Kalyani, R. Garg, R. Ranjan, Appl. Phys. Lett. 94 (2009) 202903.
[39] IEEE Standard on Piezoelectricity, ANSI/IEEE 176-1987, IEEE, New York, 1987.
[40] R.D. Shannon, Acta Crystallogr. A: Cryst. Phys. Diff. Theor. Gen. Crystallogr. 32 (1976) 751.
[41] M.A. Khan, T.P. Comyn, A.J. Bell, Acta Mater. 56 (2008) 2110.
[42] T. Qi, I. Grinberg, A.M. Rappe, Phys. Rev. B 82 (2010) 134113.
[43] K.H. Härdtl, Ceram. Int. 8 (1982) 121.